ISSN: 1844-8135 (Print); 2065-2445 (Online)
Research Article

ANNALS OF FOREST RESEARCH
www.afrjournals.org

Plant Nutrient Deficiency Detection from Leaf Images using AI/ML - driven Enhanced Channel Boosted Convolutional Neural Network

Anish Sathyan[1*] and Palanisamy P[2]

[1]Control & Instrumentation Group, C-DAC, Thiruvananthapuram, Kerala, India

[2]Department of Electronics &Communication, NIT, Tiruchirappalli, India

[*]**Corresponding Author:** Anish Sathyan**,** Control & Instrumentation Group, C-DAC, Thiruvananthapuram, Kerala, India, E-mail: satyan@cdac.in

1. Abstract

An early prediction and detection of nutrient deficiency empower farmers to appropriately categorise and apply essential nutrient supplements on time. This work presents a novel methodology built on Transfer Learning (TL) with a Convolutional Neural Network (CNN) to offer enhanced accuracy in the early detection of nutrient deficiency using leaf patterns and colour through an Enhanced Channel Boosted - Convolutional Neural Network (CB-CNN). Leaf features are extracted using Oriented FAST and Rotated BRIEF (ORB) before processing by the proposed CB-CNN. The present work precisely forecasts the type of nutrient deficiency from the leaf images, leaf pattern and leaf shape. It is observed that experimental results show 99.37% prediction accuracy over conventional neural network models. Additionally, there is considerable improvement in other performance metrics, viz., precision, specificity, sensitivity and F-score. The proposed methodology beats its existing counterparts by magnitudes ranging from 1.17% to 10.27%. It is thus clinched that the proposed model outperforms existing neural network models with the highest precision and accuracy.

2. Keywords: Plant Nutrient Deficiency; Leaf Image analysis; Bilateral filter; Channel Boosted-Convolutional Neural Network (CB-CNN); Oriented FAST and Rotated BRIEF (ORB); Transfer Learning (TL)

3. Introduction

Planet Earth's biodiversity is the predominant phenomenon in serving the global population to fulfil their agricultural and farming needs, forming the planet's most imperative nutrition source. Over centuries, nearly 7000 plant species have been found to exist on Earth. Generally, plant constituents such as seeds, flowers, leaves, bark and roots provide people with rich minerals and other nutrition compounds. Leaves feed the whole plant by absorbing sunlight, undergoing photosynthesis, producing carbohydrates and, in turn, supplying minerals and proteins. As leaves are the plant feeders, retardations in their growth induce adverse effects on plant growth and yield quantity and quality. Extensive knowledge in understanding the leaf patterns by looking for flaws in their appearance, structure, and other external features shall furnish information on healthy plants. Disease-infected leaves contribute growth retarded plants; thereby, the overall yield gets reduced. This ends up with insufficient food production cum supply causing turbulence in the net income expectations of the farmers. The nutrient deficiency of a plant can be identified well in advance by closely observing the leaf images and patterns. This non-destructive method of image processing offers a promising methodology for the masses.

Noise in an image can be reduced using a bilateral filter by integrating the spatial and range kernels, which are used to measure the respective spatial distance and intensity connected with the pixels, as explained (Zhang et al., 2014). It is described (Langampol et al. 2019) without any knowledge of the type and strength of the signal, a Smart Switching bilateral filter (SSBF) removes noise from noisy images efficiently. The inception of ResNet-v2 network architecture with transfer learning and fine-tuning processes achieves the best accuracy in detecting macronutrient deficiency of plants. The model is implemented using the okra plant image data set (Wulandhari et al. 2019).

It is found that Oriented Fast and Rotated Brief (ORB) is based on a withdrawal technique with a FAST keypoint detector. A revised version of the visual sensor (Vinay et al. 2018) focuses on providing a quick and efficient local feature detector. Kernel PCA (KPCA) is another dimensionality reduction technique covering linear uncorrelated PCA components, such as Occlusion. The published article (Partel et al. 2019) described many advanced methods, such as electrical impedance spectroscopy, reflectance spectroscopy, Fourier-transform infrared microspectroscopy and chlorophyll fluorescence spectroscopy, to gather information for deep learning. It is narrated (Azimi et al. 2021) that Nitrogen deficiency in plants reduces nutrition levels and minimizes agricultural yield. An automatic, plant-shot image-based phenotyping approach is utilized for the classification of stress stages in plants. The nitrogen concentration level in plants is vital for plant uptake and optimum agricultural yield. As described by (Elvanidi et al. 2018), three different Nitrogen concentration levels are activated in plants in a controlled greenhouse chamber, revealing the growth in crop reflection caused by nitrogen deficiency.

The reflectance spectroscopy could even detect stress manifestation and pinpointing, which can be used to produce better results, as explained (Rustioni et al. 2018). The article (Nair P et al. 2017) implemented a bilateral filter directly, which was found to be expensive. By approximating the Gaussian range kernel, a rapid and perfect approximation of the bilateral filter can be obtained using polynomials and trigonometric functions. An easy transfer learning perspective is proposed (Condori et al. 2017) using pre-trained CNN models, and those results are collated with the existing techniques in recognizing nitrogen deficiency in maize leaf images. Another method of analyzing the leaf surfaces alone is used for categorizing the presence of nutritional colour patterns present in oil palm leaves is explained (Hairuddin et al. 2011). With the help of the image shadow effect to identify the nitrogen deficiency hinge on a crop, a multi-spectral sensor was evolved to recognise the corn reflectance details from G, R, and NIR light spectra (Noh et al. 2012) established in corn plants using the shadow image. A real-time nitrogen deficiency analysis is explained (Kusumo et al. 2018) using machine learning methods like support vector machines, Decision Trees, Random Forests, and Naive Bayes to detect RGB colour information. In the automatic detection of corn diseases, local features on images being Scale-Invariant Feature Transform (SIFT), Speeded Up Robust Features (SURF), Oriented FAST and Rotated BRIEF (ORB), and Histogram of Oriented Gradients (HOG) were evaluated.

In the early stage of corn development, an Artificial Vision System (AVS) is used to recognize the levels of nitrogen deficiency. Experimental results were obtained (Romualdo et al., 2014). This indicates that the margin

of index leaves produced 82.5% Global Percentage of Right (GPR) at the V4 stage and in the bottom of old leaves 87.5% at the V7 stage in detecting nitrogen deficiency symptoms. Further, image processing approaches for RGB colour feature extraction, real-time texture, and edge detection are used with supervised machine learning to detect and identify plant nutrient deficiency (Shah et al., 2018). The hyperspectral imaging and digital image processing analysis are the popular approaches for diagnosing non-destructive nutrition in plants (Sun Y et al. 2018); these techniques are used to analyze the temporal dynamics of leaf morphology and colour. It also finds effectual in dynamic indices and optimal leaf position for recognition. Bilateral filtering is narrated (Tomasi et al. 1998) to impart smoothness to a given image while preserving its edges with the help of a nonlinear combination of neighbouring image values. The enforcement of photometric distance in the range component of the bilateral filter makes appropriate colour image processing.

This research aims to bring some novel image-processing techniques to detect nutrient deficiency by analyzing the features of leaf physiology. In digital farming, the classification of different nutrient deficiencies is a challenging task. Long-range images captured using crewless aerial vehicles (UAV), aeroplanes and satellites have been utilised to diagnose plant leaf discolouration and pattern development with the help of various techniques such as laboratory leaf analyzes and chlorophyll meters (SPAD). However, accurate and sustainable results were not possible with these discrete techniques. Mineral deficiencies of iron, magnesium, nitrogen and potassium in plants are considered to be the prime factor of stress in plants, which in turn causes a reduction in yield. The proposed effective technique of exploiting the pre-trained deep neural networks for channel-boosted convolution neural networks using oriented FAST and rotated BRIEF proves to outperform other techniques regarding accuracy and efficiency in feature extraction.

The organization of this paper is Section -II, which discusses some of the existing low-performing methodologies for identifying nutrient deficiency in a plant from leaf images. Section III details the proposed image analysis methodology using filters and an Oriented FAST and Rotated BRIEF (ORB) algorithm, improved Binary Robust Independent Elementary Feature – BRIEF implantation and Convolution Neural Network integration. Section – IV discusses the novel method of nutrient deficiency detection and analysis. The performance evaluation for the proposed system is detailed, along with various comparison charts. Conclusions are presented in section V.

4. Existing Methods

In the reference article (Xu. Z et al. 2020) (DCNN-IDNDR), different steps have been carried out to find the symptoms of nutrient deficiencies in the leaf of rice plant. Deep Convolutional Neural Network (DCNN) is the technique cast-off in image classification. Different DCNN techniques have been used to diagnose rice nutrient deficiencies and analyze the accuracy levels. Many images were collected using hydroponic experiments depicting nearly ten classes of nutrient deficiencies in plants. Four DCNN concepts, namely ResNet50, Inception-v3, NasNet-Large and DenseNet121, were used to diagnose various plant deficiencies, and the accuracies showed 90% and above, which outperforms colour feature and HOG of SVM. DenseNet121 proved with 98.62% and 97.44%. For the validation and test accuracies, respectively.

Two popular machine learning models are used (Tran et al. 2019) (CSDNN-FCMDT). Autoencoder and Inception-ResNet V2 are the models elaborated to forecast deficiencies and to classify results in 3 macronutrients, including Nitrogen, Potassium and Calcium in tomato plants. The inception module uses various hyper-parameters with various scales to identify patterns. A residual network for training the dataset was created using the Rectified Linear Unit (ReLU) activation function and Batch Normalization (BN). Batch normalization solves the vanishing gradients problem. Based on the applied images, the encoder generates internal representation and converts the rendered drawings into outputs using the pre-trained dataset decoder. The combination of Inception-ResNetV2 with auto-encoder increases the prediction accuracy of decease identification.

A new deep-learning architecture (Khatoon et al. 21) was used to classify instantly the nutritional disorders and the damages caused by pets and pathogens and their symptoms in tomato plants. A Deep Neural Network trained the proposed model. A deep CNN of different depths was introduced with the dataset of four macro-nutrient deficiencies: Potassium, Nitrogen, Calcium, and Magnesium. Other disease classes and nutritional disorders were compared using deep learning architecture like VGGNet-16, DenseNet and ResNet and prediction accuracy was calculated and compared.

The leaf images were divided into minor blocks in the article (Watchareeruetai et al. 2018) (IDPND-CNN). Each block of leaf pixels was applied to a set of CNNs that responded if an identified block had nutrient deficiency symptoms. A multi-layer perception network integrates all the responses from every block into one to produce final results for detecting nutrient deficiency.

5. Proposed Methods

The deep learning-based proposed method uses a Bilateral filter in the first stage to eliminate the redundant content in input images.

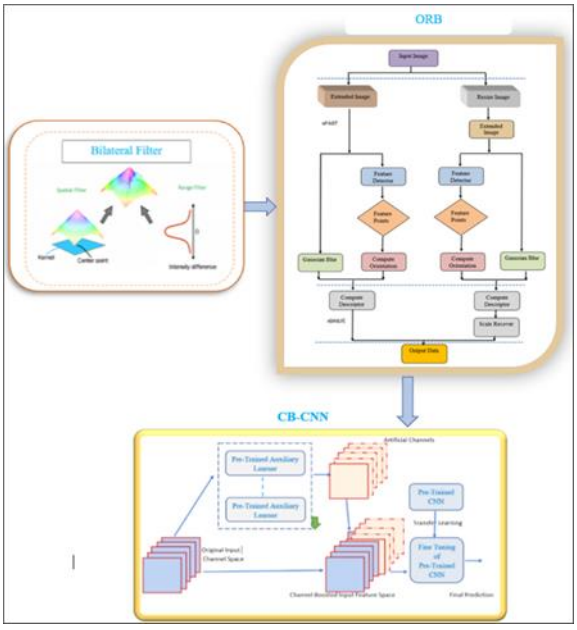

Figure 1: Proposed model of enhanced ORB-CBCNN.

Then, ORB is used to extract the key features from filtered images. In the last step, CR-CNN is used to classify the output more accurately. The process flow of the proposed method is shown in Figure 1.

5.1. Smoothening filter

The noise-reducing smoothening filter called the Bilateral Non-linear filter, which preserves edge information from input leaf images, is used in this work. A weighted average value from neighbouring pixels replaces all the intensity values of pixels. Gaussian distribution is used in finding the weighted average of images. The calculated weights are based not only on pixels' Euclidean distance but also applied to the range differences such as instance colour intensity, depth distance, etc. Thus, in the enhanced method, the sharp edges are preserved by properly looping all pixels through weight adjustments.

A bilateral filter defined by Tomasi et al. (1998) [17] and Banterle et al. (2012) [22] is given by

$$I_F(d) = \frac{1}{N_p}\sum_{d_i \in \emptyset} I(d_i) g_r(\|I(d)_i - I(d)\|) g_s(\|d_i - d\|) \quad (1)$$

Normalization factor Np is given by,

$$N_P = \sum_{d_i \in \emptyset} g_r(\|I(d_i) - I(d)\|) g_s(\|d_i - d\|) \quad (2)$$

Where,

$I_F \rightarrow Output\ of\ the\ filter - filtered\ image$

$d \rightarrow coordinates\ of\ the\ present\ pixel$

$\emptyset \rightarrow window\ centered\ in\ d\ so\ d_i \in \emptyset\ is\ the\ next\ pixel$

$g_r \rightarrow\ kernel\ range\ for\ smoothing\ differences$

$g_s \rightarrow kernel\ spatial\ for\ smoothining\ differences$

The weight N_P is calculated by spatial closeness(g_s) and intensity differences (g_r)

In an image, consider a pixel at (x, y), which is to be denoised using its nearby pixels and assume a pixel at (i, j) as its neighbouring pixel. Then, assume a Gaussian kernel as range and spatial kernel, to remove the noise in the pixel (x, y) , the assigned weight at (i, j) is

the weight assigned for pixel (i, j) is given by

$$w(x, y, i, j) = \exp\left(-\frac{(x-i)^2+(y-j)^2}{2\sigma_g^2} - \frac{\|I(x,y)-I(i,j)\|^2}{2\sigma_r^2}\right) \quad (3)$$

$\sigma_g\ and\ \sigma_{r \rightarrow smoothing\ parameter}$

$I(x, y) and\ I(i, j) are\ the\ intensity\ pixels\ of$

$(x, y) and\ (i, j) respectively$

Normalize them after calculating the weights

$$I_D(x,y) = \frac{\sum_{i,j} I(i,j) w(x,y,i,j)}{\sum_{x,y} w(x,y,i,j)} \quad (4)$$

$$I_D \rightarrow denoised\ intensity\ of\ pixel(x,y)$$

5.2. Oriented FAST and Rotated BRIEF (ORB) algorithm

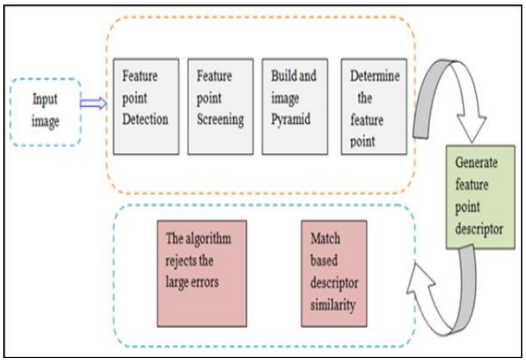

Figure 2: Flow diagram of ORB algorithm.

The flow diagram of the ORB algorithm, an alternative to the SIFT (Scale-Invariant Feature Transform) and SURF (Speeded-Up Robust Features) methods, is shown in Figure 2. It improves efficiency of the system. The method ORB will perform best with the help of the FAST key point detector and the BRIEF descriptor.

The essential features of ORB are

i. The summation of fast and correct orientation items to FAST
ii. The oriented BRIEF attributes computation is efficient.
iii. It will investigate the correlation and variance of oriented BRIEF features.
iv. A data-acquiring method for decorrelating BRIEF features will give the finer presentation in the nearest neighbour applications.

5.3. Features extraction using Accelerated and Segments Tests (FAST)

A single image is represented as a multiscale image pyramid, which is arranged as a sequence with different resolutions (downsampled). The key point of the image is detected with the help of a pyramid. Once the key point is detected then, ORB assigns the orientation of the key points based on the level of intensity. Figure 3 shows the Multiscale image pyramid method used in the ORB algorithm.

Considering a pixel p in an array of images, the FAST algorithm compares the brightness of the 16 pixels, which are in a small circle around the pixel p. The pixels in the small circle are again sorted into three types: lighter than p, darker than p or similar to pixel p. The critical point is selected based on the pixels in the circle when above eight pixels are brighter or darker than p.

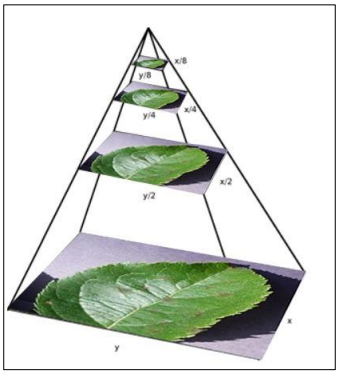

Figure 3: Multiscale Image Pyramid.

ORB measures corner orientation

The ORB descriptor- Patch's definition is given below

$$Z_{xy=\sum_{ab} a^x b^y I(a,b)} \quad (5)$$

After calculating the above instance the patch's centroid, the "center of mass" is given by

$$C=\left(\frac{Z_{10}}{Z_{00}}\frac{Z_{01}}{Z_{00}}\right) \quad (6)$$

The corner's center O implements a new improved vector to the centroid - OC. Hence, the closeness subscript direction of the patch is specified by:

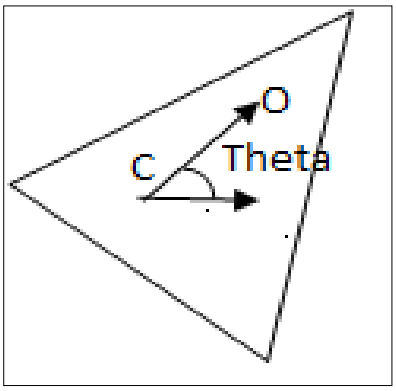

Figure 4: Angle (θ) calculation.

The angle calculation is illustrated in Figure 4.

$$\theta = a\tan 2\,(Z_{01}Z_{10}) \quad (7)$$

Once the orientation of the patch is identified, then the patch can be rotated like canonical rotation. So, the descriptor value can be calculated, which is obtained with some invariance in rotation.

3.4 Binary Robust Independent Elementary Feature – BRIEF

Here, BRIEF and FAST are used to represent the object together. The output of the FAST algorithm is given to the BRIEF. The FAST algorithm helps to find all the key points. BRIEF will convert the Binary Feature Vectors (BFV) of all critical points. BFV, also called Binary Feature Descriptor (BFD), contains only 1 and 0. Therefore, every key point is introduced by a feature vector of 128-512 bits string. ORB adds this feature without reducing the speed factor of BRIEF.

Let P be the patch of the smoothed image. A binary test τ(P; a, b) is now defined as

$$\tau(P;a,b) = \begin{cases} 1, P(a) < P(y) \\ 0, P(a) \geq P(b) \end{cases} \quad (8)$$

P(a) is the intensity value at pixel a

where P(a) represents intensity of P at the point a. Now, the vector of n binary tests, F(n), is described as

$$F(n) = \sum_{1<i<n} 2^{i-1} \tau\ (P;\ a^i b^i, b) \quad (9)$$

The complementing performance of BRIEF reduces abruptly for in-plane rotation of angles more than a few degrees. ORB proposes a technique to guide BRIEF as stated by the orientation of the key points. For n binary tests with any attribute set at location (xi, yi), a 2 x n matrix can be written as

$$S=\begin{bmatrix} a1 \ldots \ldots a_n \\ b1 \ldots \ldots b_n \end{bmatrix} \quad (10)$$

It utilizes the orientation θ of a patch P and Rθ, the correlated rotation matrix, and set up a guided part Sθ of S:

$$S_\theta = R_{\theta s} \quad (11)$$

Hence, the guided BRIEF operator can be given by

$$g_n\ (p, \theta) = f_n(\mathrm{p}) |\ (a_i b_i\ ) \in S_\theta \quad (12)$$

Then the angle is sampled to change into discrete format with an interval of 2π/30 (12 degrees), and a lookup table is created with pre-calculated BRIEF features. The guided points Sθ will calculate the descriptor until the key point θ is orientated and viewed consistently.

5.5. Enhanced Channel Boosted-Convolutional Neural Networks

Here the output of the ORB is given to the newly developed Auxiliary Learner, which consists of the Auto Encoder, and to the other side to reduce the dimensionality. The advantage of the architecture is managing the different information of the image at various spatial resolutions. The sparsity in the network is introduced to reduce the computational cost because of parallel processing. The working procedure of CB-CNN is shown in Figure 5. Finally, the proposed methodology accurately predicts the nutrient deficiency of the plant, and it displays the Nitrogen level of the corresponding leaf. Four main plant leaves (salad cucumber, tomato, corn, and rice) are trained and used for nutrient deficiency prediction.

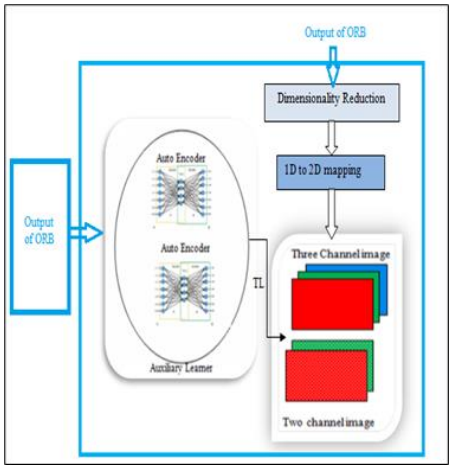

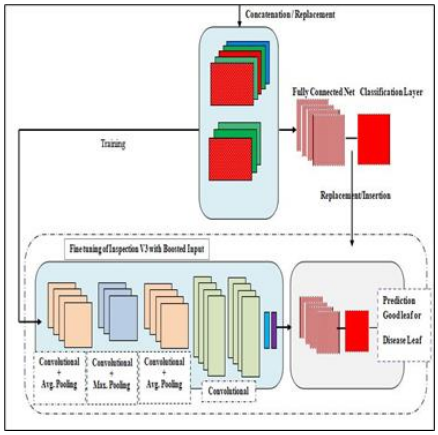

Figure 5a, 5b: Enhanced CB-CNN working flow diagram.

The following novel methodologies are designed and implemented in this work:

- To improve the representational capacity of the Convolutional Neural Networks, a new Channel Boosted method is introduced.
- The Channel Boosting method is incorporated with CNN and can apply complex classification problems by predicting even minor differences between the images.
- The proposed method works with both transfer learning and input images.
- The representation of input images is boosted by generating various images obtained through transfer learning and deep generative learners.

6. Results and Discussion

The output images of Rice leaf are shown in Figure 6 after every stage of the proposed method. Figures 6, 7, 8 and 9 show Rice, Apple and Blueberry leaves with their nitrogen levels. Generally, if the nitrogen level is high, then the leaf and the whole plant are considered to be healthy; if the nitrogen value is reduced, the deficiency can be identified based on the leaf discolouration. The leaf becomes pale green due to nitrogen deficiency.

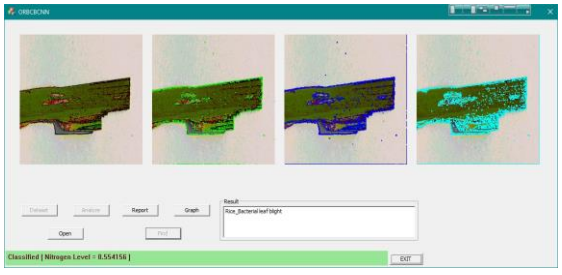

Figure 6: Rice_Bacteral leaf blight with nitrogen level of 0.554156.

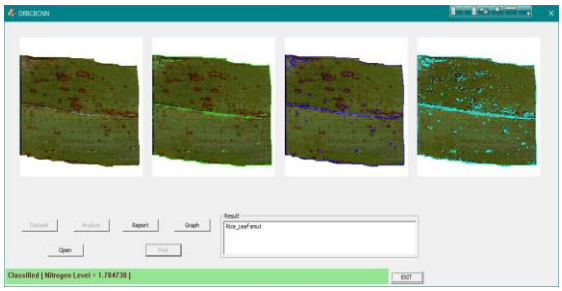

Figure 7: Rice_ leaf smut with a nitrogen level of 1.784738.

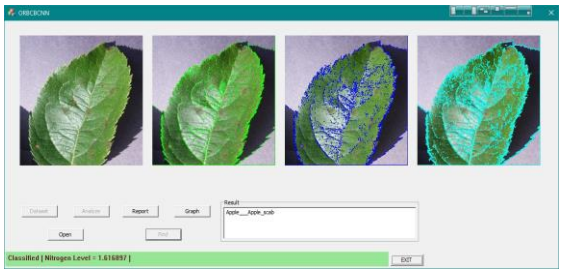

Figure 8: Apple_Scab with the nitrogen level of 1.61689.

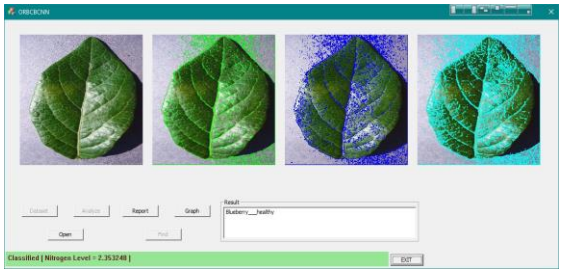

Figure 9: Buleberry_Healthy leaf with nitrogen level of 2.353248.

6.1. Accuracy (ACC) in percentage

Accuracy is the ratio of the correct prediction to the total predictions.

$$ACC = \frac{TP + TN}{TP + FN + FP + TN} * 100$$

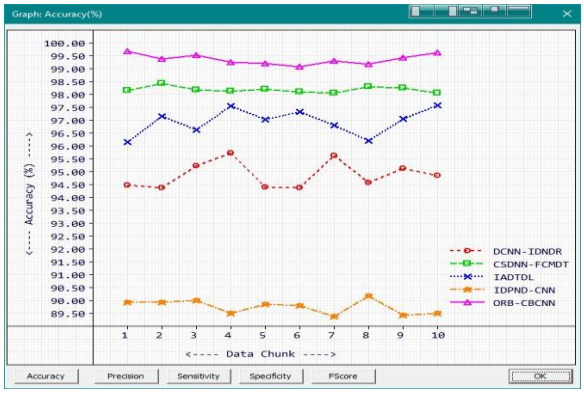

Figure 10: Accuracy comparison chart.

Table 1 and Figure 10 depict that the proposed ORB-CBCNN methodology provides improved performance in accuracy than the DCCNN-IDNDR, CDCNN-FCMDT, IADTDL and IDPND-CNN with the percentage difference of 4.62%, 1.19%, 2.46% and 10.17% respectively.

Table 1: Accuracy in percentage.

6.2. Precision (PREC)

The sensitivity percentage is calculated based on the number of correct optimistic predictions divided by the sum of positive predictions.

$$SN = \frac{Correct\ Positive\ Prediction\ (TP)}{TP + FP} * 100$$

Table 2 and Figure 11 indicates that the proposed ORB-CBCNN methodology provides improved performance in precision than the DCCNN-IDNDR, CDCNN-FCMDT, IADTDL and IDPND-CNN with the percentage difference of 4.62%, 1.19%, 2.46% and 10.17% respectively.

Data Chunk	CSDNN-IDNDR	CSDNN-FCMDT	LADTDL	IDPND-CNN	ENHANCED ORB-CBCNN
1	94.490005	98.160004	96.169998	89.93	99.684998
2	94.395004	98.445	95.150002	89.945	99.375
3	95.229996	98.184998	96.645004	90.004997	99.544998
4	95.725006	99.145004	97.57	89.5	99.25
5	94.405006	98.224998	97.040001	89.860001	99.220001
6	94.375	98.104996	97.334999	89.815002	99.095001
7	96.635002	98.065002	96.809998	89.395004	99.324997
8	94.599998	98.320007	96.220001	90.190002	99.18
9	95.144997	98.269997	97.055	89.43	99.43
10	94.870003	98.060005	97.584999	89.519997	99.630005
Average	**94.8870017**	**98.1980011**	**96.9580002**	**89.7590003**	**99.3735**

Table 2: Resulted Precision in the percentage.

Data Chunk	CSDNN-IDNDR	CSDNN-FCMDT	LADTDL	IDPND-CNN	ENHANCED ORB-CBCNN
1	94.857834	98.208206	95.460808	90.538071	99.759644
2	94.047028	98.459534	97.112312	89.877213	99.360191
3	95.475563	98.267052	95.370094	90.242432	99.431305
4	95.922470	98.159447	96.655548	89.202065	99.102692
5	94.311943	98.316803	96.280991	90.409569	99.318634
6	94.229042	98.148331	96.365952	90.392616	99.070465
7	95.612190	98.079422	96.118225	89.335999	99.094254
8	94.986885	98.233185	95.393829	90.694611	99.248947
9	95.086388	98.327995	97.097382	89.210419	99.748390
10	94.549248	98.079231	96.601700	89.814629	99.600235
Average	**94.9078591**	**98.2279206**	**96.245684**	**89.9717624**	**99.3734757**

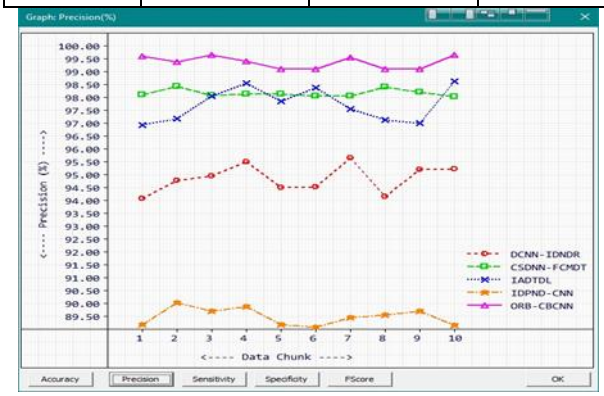

Figure 11: Precision for different methods.

6.3. Sensitivity (SN)

The percentage of sensitivity is calculated based on the number of correct optimistic predictions divided by the total accurate prediction

$$SN = \frac{Correct\ Positive\ Prediction\ (TP)}{TP + FN} * 100$$

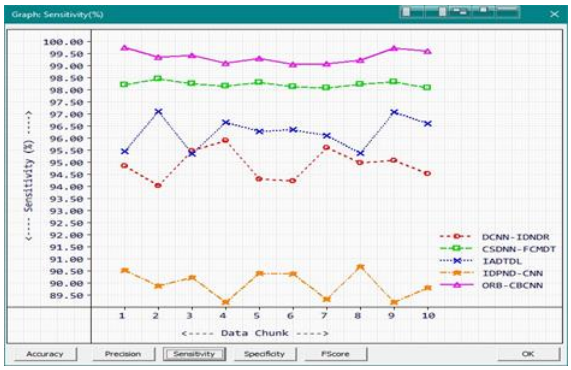

Figure 12: Precision for different methods

Table 3 and Figure 12 expose that the proposed ORB-CBCNN methodology provides improved performance in sensitivity than the DCCNN-IDNDR, CDCNN-FCMDT, IADTDL and IDPND-CNN with the percentage difference of 4.62%, 1.19%, 2.46% and 10.17% respectively.

Data Chunk	CSDNN-IDNDR	CSDNN-FCMDT	LADTDL	IDPND-CNN	ENHANCED ORB-CBCNN
1	94.080002	98.110001	96.949997	89.18	99.610001
2	94.790001	98.43	97.190002	90.029999	99.389999
3	94.959999	98.099998	98.050003	89.709999	99.660004
4	95.510002	98.129997	98.550003	89.879997	99.400002
5	94.510002	98.129997	97.860001	89.180000	99.120003
6	94.540001	98.059998	98.379997	89.099998	99.120003
7	95.660004	98.050003	97.559998	89.470001	,99.559998
8	,94.169998	98.410004	97.129997	89.570000	99.110001
9	95.209999	98.209999	97.010002	89.709999	99.110001
10	95.230003	98.040001	98.639999	89.150002	99.660004
Average	**94.8660011**	**98.1669998**	**97.732**	**89.47979995**	**99.3740016**

Table 3: Sensitivity is calculated in percentage.

6.4. F-Score

F-Score represents the harmonic mean of precision and sensitivity. It is measured as mentioned below:

$$F - Score = \frac{2 * PREC * SN}{PREC + SN}$$

Table 4 and Figure 13 show that the proposed ORB-CBCNN methodology provides improved performance in

Data Chunk	CSDNN-IDNDR	CSDNN-FCMDT	LADTDL	IDPND-CNN	ENHANCED ORB-CBCNN
1	94.467323	98.159081	96.199638	89.853897	99.684769
2	94.417046	98.444771	97.151146	89.953545	99.375092
3	95.217087	98.183456	96.691483	89.975433	99.545525
4	95.715797	98.144722	97.593582	89.539749	99.251129
5	94.410866	98.223305	97.064072	89.790581	99.219215
6	94.384270	98.104141	97.362564	89.741653	99.095238
7	95.636101	98.064713	96.833748	89.402954	99.326576
8	94.576675	98.321510	96.254082	90.128792	99.179428
9	95.148155	98.268959	97.053665	89.459511	99.428169
10	94.888397	98.059608	97.610214	89.481079	99.630112
Average	**94.8861717**	**98.1974266**	**96.981419**	**89.7327194**	**99.3735253**

F-Score than the DCCNN-IDNDR, CDCNN-FCMDT, IADTDL and IDPND-CNN with the percentage difference of 4.62%, 1.19, %, 2.46% and 10.17% respectively.

Table 4: Calculated F-Score.

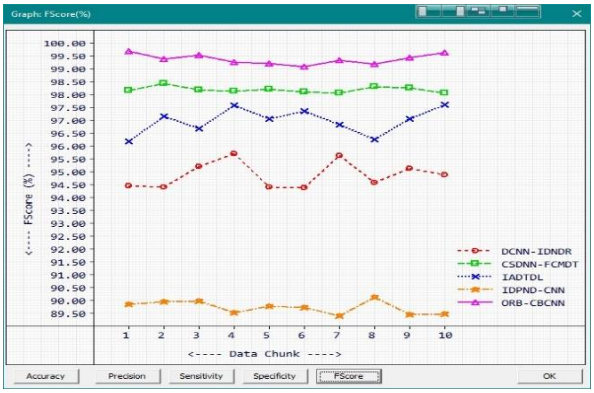

Figure 13: F-Score for different methods.

7. Conclusions

Here a novel hybrid variant with an Enhanced Convolutional Neural Network is introduced along with ORB-CBCNN to increase the prediction accuracy of plant leaf classifiers. At first, all noises from the input plant dataset are removed using a bilateral filter. Next, the filtered dataset is driven through the proposed Oriented FAST and Rotated BRIEF (ORB) algorithm for leaf feature extraction. Finally, the extracted features are carried across the enhanced CB-CNN classifier that classifies leaf quality into normal, healthy or nutrient deficient. Here, the proposed model is efficiently designed and implemented to classify nutrient-deficient plants using leaf color and pattern. The enhanced ORB-CBCNN model performance is evaluated by incorporating a plant village dataset of metrics viz., Accuracy, Precision, Specificity, Sensitivity, and F-Score. The introduced model employed transfer learning (TL) and CNN together to deliver impressive performance in the case of any plant

leaf. The proposed ORB-CBCNN-based methodology outperformed its counterparts with a percentage difference of 4.62%, 1.19%, 2.46% and 10.17%, respectively, regarding all CNN metrics.

Acknowledgements

We sincerely thank the International Plant Nutrient Institute (IPNI) & Plant Village for the dataset. The nutrient-deficient dataset of IPNI is augmented with the plant village dataset to create the dataset for the purpose of study.

Ethical statement

All ethical practices have been followed in relation to the development, writing, and publication of the paper.

Declaration of Competing Interest

The authors declare that they have no known competing financial interests or personal relationships that could have appeared to influence the work reported in this paper.

References

1. Zhang Y., Tian X., Ren P., 2014. An adaptive bilateral filter-based framework for image denoising. Neurocomputing 140: 299-316.
2. Langampol K., Srisomboon K., Patanavijit V., Lee W., 2019. Smart switching bilateral filter with estimated noise characterization for mixed noise removal. Mathematical Problems in Engineering.
3. Wulandhari L.A., Gunawan A.A.S., Qurania A., Harsani P., Tarawan T.F., Hermawan R.F., 2019. Plant nutrient deficiency detection using deep convolutional neural network. ICIC Express Letters 13(10): 971-977.
4. Vinay A., Cholin A.S., Bhat A.D., Murthy K.B., Natarajan S., 2018. An efficient ORB-based face recognition framework for human-robot interaction. Procedia computer science 133: 913-923.
5. Partel V., Nunes L., Stansly P., Ampatzidis Y., 2019. Automated vision-based system for monitoring Asian citrus psyllid in orchards utilizing artificial intelligence. Computers and Electronics in Agriculture 162: 328-336.
6. Azimi S., Kaur T., Gandhi T.K., 2021. A deep learning approach to measure stress level in plants due to nitrogen deficiency. Measurement 173: 108650.
7. Elvanidi A., Katsoulas N., Augoustaki D., Loulou I., Kittas C., 2018. Crop reflectance measurements for nitrogen deficiency detection in a soilless tomato crop. Biosystems Engineering 176: 1-11.
8. Rustioni L., Grossi D., Brancadoro L., Failla O., 2018. Iron, magnesium, nitrogen and potassium deficiency symptom discrimination by reflectance spectroscopy in grapevine leaves. Scientia Horticulturae 241: 152-159.
9. Nair P., Popli A., Chaudhury K.N., 2017. A fast approximation of the bilateral filter using the discrete Fourier transform. Image Processing on Line 7: 115-130.
10. Condori R.H.M., Romualdo L.M., Bruno O.M., de Cerqueira Luz P.H., 2017. Comparison between traditional texture methods and deep learning descriptors for detecting nitrogen deficiency in maize crops. In 2017 Workshop of Computer Vision (WVC) pp: 7-12.

11. Hairuddin M.A., Tahir N.M., Baki S.R.S., 2011. Overview of image processing approach for nutrient deficiencies detection in Elaeis Guineensis. In 2011 IEEE international conference on system engineering and Technology pp: 116-120.

12. Noh H., Zhang Q., 2012. Shadow effect on multi-spectral image for detection of nitrogen deficiency in corn. Computers and electronics in agriculture 83: 52-57.

13. Kusumo B.S., Heryana A., Mahendra O., Pardede H.F., 2018. Machine learning-based for automatic detection of corn-plant diseases using image processing. In 2018 International Conference on Computer, Control, Informatics and its Applications (IC3INA) pp: 93-97.

14. Romualdo L.M., Luz P.H.C., Devechio F.F.S., Marin M.A., Zúñiga A.M.G., et al. 2014. Use of artificial vision techniques for diagnostic of nitrogen nutritional status in maize plants. Computers and electronics in agriculture 104: 63-70.

15. Shah A., Gupta P., Ajgar Y.M. 2018. Macro-Nutrient Deficiency Identification in Plants Using Image Processing and Machine Learning. In 2018 3rd International Conference for Convergence in Technology (I2CT) pp: 1-4.

16. Sun Y., Tong C., He S., Wang K., Chen L., 2018. Identification of nitrogen, phosphorus, and potassium deficiencies based on temporal dynamics of leaf morphology and color. Sustainability 10(3): 762.

17. Tomasi C., Manduchi R., 1998. Sixth International Conference on Computer Vision. Bombay pp: 839-846.

18. Xu Z., Guo X., Zhu A., He X., Zhao X., et al. 2020. Using Deep Convolutional Neural Networks for Image-Based Diagnosis of Nutrient Deficiencies in Rice. Computational Intelligence and Neuroscience.

19. Tran T.T., Choi J.W., Le T.T.H., Kim J.W., 2019. A comparative study of deep CNN in forecasting and classifying the macronutrient deficiencies on development of tomato plant. Applied Sciences 9(8): 1601.

20. Khatoon S., Hasan M.M., Asif A., Alshmari M., Yap Y., 2021. Image-based automatic diagnostic system for tomato plants using deep learning. Computers, Materials & Continua 67(1): 595-612.

21. Watchareeruetai U., Noinongyao P., Wattanapaiboonsuk C., Khantiviriya P., Duangsrisai S., 2018. Identification of plant nutrient deficiencies using convolutional neural networks. In 2018 International Electrical Engineering Congress (iEECON) pp: 1-4.

22. Banterle F., Corsini M., Cignoni P., Scopigno R., 2012. A low-memory, straightforward and fast bilateral filter through subsampling in the spatial domain. In Computer Graphics Forum 31(1): 19-32.